Multi-Aperture Digital Coherent Combining for Free-Space Optical Communication Receivers

David J. Geisler*, Timothy M. Yarnall, Mark L. Stevens, Curt M. Schieler, Bryan S. Robinson, and Scott A. Hamilton

Optical Communications Technology, MIT Lincoln Laboratory, 244 Wood St., Lexington, MA 02421, USA
*david.geisler@ll.mit.edu

Abstract: Space-to-ground optical communication systems can benefit from reducing the size, weight, and power profiles of space terminals. One way of reducing the required power-aperture product on a space platform is to implement effective, but costly, single-aperture ground terminals with large collection areas. In contrast, we present a ground terminal receiver architecture in which many small less-expensive apertures are efficiently combined to create a large effective aperture while maintaining excellent receiver sensitivity. This is accomplished via coherent detection behind each aperture followed by digitization. The digitized signals are then combined in a digital signal processing chain. Experimental results demonstrate lossless coherent combining of four lasercom signals, at power levels below 0.1 photons/bit/aperture.

OCIS codes: (060.1660) Coherent communications; (070.2025) Discrete optical signal processing; (060.2605) Free-space optical communication; (060.5060) Phase modulation.

References and links

1. D. M. Boroson, B. S. Robinson, D. V. Murphy, D. A. Burianek, F. Khatri, J. M. Kovalik, Z. Sodnik, and D. M. Cornwell, "Overview and results of the lunar laser communications demonstration," in *Proc. SPIE 8971, Free-Space Laser Communication and Atmospheric Propagation XXVI, 89710S*, (2014).
2. D. M. Cornwell, "NASA's optical communications program for 2015 and beyond," in *Proc. SPIE 9354, Free-Space Laser Communication and Atmospheric Propagation XXVII, 93540E*, (2015).
3. R. W. Kingsbury, D. O. Caplan, and K. L. Cahoy, "Compact optical transmitters for cubesat free-space optical communications," in *Proc. SPIE 9354, Free-Space Laser Communication and Atmospheric Propagation XXVII, 93540S*, (2015).
4. H. Hemmati, *Deep Space Optical Communications* (John Wiley & Sons, Inc., Hoboken, New Jersey, 2006).
5. D. O. Caplan, "Laser communication transmitter and receiver design," J. Opt. Fiber. Commun. **4**(4-5), 225-362 (2007).
6. H. Hemmati and D. O. Caplan, "Optical Satellite Communications," in *Optical Fiber Telecommunications,* Sixth ed., I. P. Kaminow, T. Li, and A. E. Willner, eds. (Elsevier, 2013).
7. S. B. Alexander, *Optical Communication Receiver Design* (SPIE, 1997).
8. D. M. Boroson, "A survey of technology-driven capacity limits for free-space laser communications," in *Proc. SPIE 6709, Free-Space Laser Communications VII, 670918*, (2007).
9. X. Liu, T. H. Wood, R. W. Tkach, and S. Chandrasekhar, "Demonstration of record sensitivities in optically preamplified receivers by combining PDM-QPSK and m-ary pulse-position modulation," J. Lightw. Technol. **30**(4), 406-413 (2012).
10. D. J. Geisler, T. M. Yarnall, W. E. Keicher, M. L. Stevens, A. S. Fletcher, R. R. Parenti, D. O. Caplan, and S. A. Hamilton, "Demonstration of 2.1 photon-per-bit sensitivity for BPSK at 9.94-Gb/s with rate-1/2 FEC," in *Proceedings of Optical Fiber Communications Conference (OFC)*, (2013), paper OM2C.6.
11. D. J. Geisler, V. Chandar, T. M. Yarnall, M. L. Stevens, and S. A. Hamilton, "Multi-gigabit coherent communications using low-rate FEC to approach the Shannon capacity Limit," in *Conference on Lasers and Electro-Optics (CLEO)*, (2015), paper SW1M.2.
12. P. H. Stahl, "Survey of cost models for space telescopes," Optical Engineering **49**(5), 053005 (2010).
13. S. Shaklan and F. Roddier, "Coupling starlight into single-mode fiber optics," Appl. Opt. **27**(11), 2334-2338 (1988).

14. V. Jamnejad, J. Huang, B. Levitt, T. Pham, and R. Cesarone, "Array antennas for JPL/NASA Deep Space Network," in *Proceedings of IEEE Aerospace Conference Proceedings*, vol. 2 911-921, (2002).
15. J. M. Hill, "The Large Binocular Telescope," Appl. Opt. **49**(16), D115-D122 (2010).
16. V. W. S. Chan, "Optical satellite networks," J. Lightw. Technol. **21**(11), 2811-2827 (2003).
17. J. Ma, K. Li, L. Tan, S. Yu, and Y. Cao, "Performance analysis of satellite-to-ground downlink coherent optical communications with spatial diversity over Gamma–Gamma atmospheric turbulence," Appl. Opt. **54**(25), 7575-7585 (2015).
18. A. Belmonte and J. M. Kahn, "Array receivers in downlink coherent lasercom," in *Proc. SPIE 9354, Free-Space Laser Communication and Atmospheric Propagation XXVII, 935407*, (2015).
19. J. Xu, A. Delaval, R. G. Sellar, A. Al-Habash, P. Reardon, R. L. Phillips, and L. C. Andrews, "Experimental comparison of coherent array detection and conventional coherent detection for laser radar and communications," in *Proc. SPIE 3615, Free-Space Laser Communication Technologies XI, 54*, 54-63, (1999).
20. A. R. Weeks, J. Xu, R. R. Phillips, L. C. Andrews, C. M. Stickley, G. Sellar, J. S. Stryjewski, and J. E. Harvey, "Experimental verification and theory for an eight-element multiple-aperture equal-gain coherent laser receiver for laser communications," Appl. Opt. **37**(21), 4782-4788 (1998).
21. C. M. Stickley, R. Phillips, A. Weeks, and P. Gatt, "Demonstration of an adaptive, coherent-combining laser radar receiver," in *Advances in Atmospheric Remote Sensing with Lidar* (Springer Berlin Heidelberg, 1997), pp. 247-250.
22. P. Gatt, T. P. Costello, D. A. Heimmermann, D. C. Castellanos, A. R. Weeks, and C. M. Stickley, "Coherent optical array receivers for the mitigation of atmospheric turbulence and speckle effects," Appl. Opt. **35**(30), 5999-6009 (1996).
23. X. Liu, S. Chandrasekhar, P. Winzer, A. Chraplyvy, B. Zhu, T. Taunay, and M. Fishteyn, "Performance improvement of space-division multiplexed 128-Gb/s PDM-QPSK signals by constructive superposition in a single-input-multiple-output configuration," in *Proceedings of Optical Fiber Communication Conference (OFC)*, (2012), paper OTu1D.3.
24. X. Liu, S. Chandrasekhar, A. H. Gnauck, P. J. Winzer, S. Randel, S. Corteselli, A. R. Chraplyvy, R. W. Tkach, B. Zhu, T. F. Taunay, and M. Fishteyn, "Digital coherent superposition for performance improvement of spatially multiplexed coherent optical OFDM superchannels," Opt. Express **20**(26), B595-B600 (2012).
25. T. M. Yarnall, D. J. Geisler, M. L. Stevens, C. M. Schieler, B. S. Robinson, and S. A. Hamilton, "Multi-aperture digital coherent combining for next-generation optical communication receivers," in *Proc. 2015 International Conference on Space Optical Systems and Applications (ICSOS), 1570211585*, (2015).
26. B. Jalali and S. Fathpour, "Silicon photonics," J. Lightw. Technol. **24**(12), 4600-4615 (2006).
27. A. Leven, N. Kaneda, and S. Corteselli, "Real-time implementation of digital signal processing for coherent optical digital communication systems," IEEE J. Sel. Topics Quantum Electron. **16**(5), 1227-1234 (2010).
28. S. Meint, L. Xaveer, A. Huub, B. Erwin, T. Jos van der, S. Barry, *et al.*, "An introduction to InP-based generic integration technology," Semicond. Sci. Technol. **29**(8), 083001 (2014).
29. R. Tyson, *Principles of Adaptive Optics,* 3rd ed. (CRC Press, Boca Raton, FL, 2011).
30. P. J. Winzer and W. R. Leeb, "Fiber coupling efficiency for random light and its applications to lidar," Opt. Lett. **23**(13), 986-988 (1998).
31. N. Cvijetic, S. G. Wilson, and M. Brandt-Pearce, "Receiver optimization in turbulent free-space optical MIMO channels with APDs and Q-ary PPM," IEEE Photon. Technol. Lett. **19**(2), 103-105 (2007).
32. F. G. Walther, J. D. Moores, R. J. Murphy, S. Michael, and G. A. Nowak, "A process for free-space laser communications system design," in *Proc. SPIE 7464, Free-Space Laser Communications IX, 74640V*, (2009).
33. M. Morelli and U. Mengali, "Feedforward frequency estimation for PSK: A tutorial review," Eur. Trans. Telecommun. **9**(2), 103-116 (1998).
34. T. Pfau, S. Hoffmann, and R. Noé, "Hardware-efficient coherent digital receiver concept with feedforward carrier recovery for m-QAM constellations," J. Lightw. Technol. **27**(8), 989-999 (2009).
35. "Digital Video Broadcasting (DVB); second generation framing structure, channel coding and modulation systems for broadcasting, interactive services, news gathering and other broadband satellite applications (DVB-S2)," in *ETSI EN 302 307 V1.2.1 (2009-08),* (European Telecommunications Standards Institute (ETSI), 2009).
36. J. Davis and W. J. Tango, "Measurement of the atmospheric coherence time," Publications of the Astronomical Society of the Pacific **108**(723), 456-458 (1996).

1. Introduction

Future space platforms, whether they are near-Earth satellites or probes to the moon or other planets, must provide communication back to the Earth that can deliver a large data volume without significantly impacting the size, weight, and power (SWaP) available for the primary mission payload [1-3]. Free space optical (FSO) communication links can provide high data rates by exploiting the unregulated and nearly unlimited amount of bandwidth available in the infrared portion of the electromagnetic spectrum [4, 5]. The SWaP of space-borne lasercom downlink terminals is driven in a large part by the power-aperture product

required to close the link [6]. For many years, SWaP reduction efforts focused on creating ground receivers with excellent sensitivity [5, 7]. This was achieved through judicious combination of modulation format, forward error correction (FEC), and high-performance photo-detection with low implementation loss. Recent results have demonstrated receiver sensitivities within a few dB of the theoretical performance limits [8-11]. One way to continue the reduction of space-side terminal SWaP is to create a ground receiver with a large effective collection area.

The obvious means to increasing collection area for single aperture ground terminals is to increase the aperture diameter. However, optical telescopes with apertures larger than a few 10's of centimeters are very expensive and difficult to build – a different approach is needed [12]. Furthermore, atmospheric turbulence adds to the difficulty of coupling light from large telescopes into optical fiber [13]. Another approach for increasing collection area is to combine signals from multiple apertures. The concept of using multiple receive apertures to increase collection area has been successfully demonstrated in radio frequency (RF) systems (*e.g.*, the NASA Deep-Space Network (DSN) [14]) and optical imaging telescopes (*e.g.*, Large Binocular Telescope Observatory (LBTO) [15]). Large monolithic telescope apertures, however, have difficulty pointing near the sun or operating during the day due to thermal heating issues. Multiple receive apertures have also been demonstrated in *incoherent* optical systems (*e.g.*, NASA Lunar Laser Communications Demonstration (LLCD) [1]). Although sytems such as LLCD can achieve excellent sensitivity by using single-photon detectors, these solutions are custom, limited to 100's Mb/s data rates, and require cryogenic stabilization of the detectors.

Theoretical analysis and experimental demonstrations of optical *coherent* combining have been investigated as a means for mitigating atmospheric effects [16-18] for communications and laser radar applications [19-22]. These initial demonstrations relied on analog approaches to coherent combining including optical phase-locked loops (OPLL) and fiber variable phase delays. Coherent combining can also be implemented digitally by using digital coherent receivers and digital signal processing (DSP), which eliminates the need for OPLLs and optical phase shift hardware for phase alignment. In particular, recent fiber experiments targeting nonlinear transmission impairment mitigation have shown successful digital optical coherent combining [23, 24]. These demonstrations involved transmitting a common signal through the multiple spatial modes of a multi-core optical fiber which were then combined at the receiver using digital coherent techniques. However, a practical and scalable implementation of digital optical coherent combining for multi-aperture FSO communications has yet to be experimentally demonstrated.

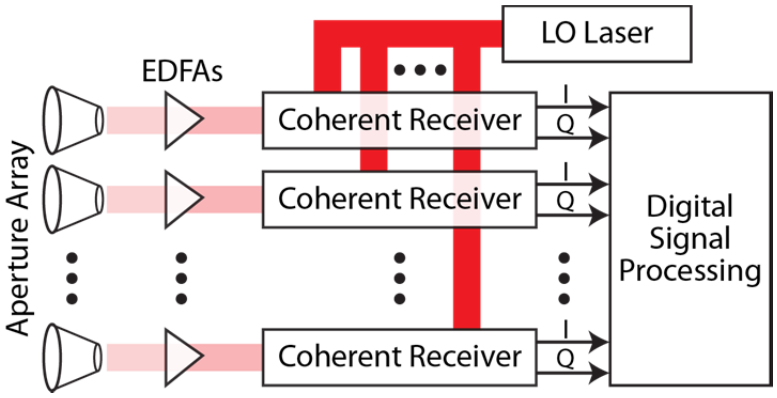

Fig. 1. Digital optical coherent combining architecture. EDFA: erbium-doped fiber amplifier. LO: local oscillator.

We report experimental results demonstrating that coherent combining of multiple apertures can be efficiently implemented while maintaining excellent receiver sensitivity, extending the results of our prior research [25]. Fig. 1 shows the general architecture for implementing digital coherent combining of signals from different apertures. In this approach, multiple apertures receive versions of the same signal that have each experienced independent atmosphere-induced intensity and phase variations. The received signals then propagate through parallel preamplified coherent receiver chains that all share a common local oscillator (LO). Next, the in-phase (*I*) and quadrature-phase (*Q*) components from each receiver are digitized, temporally aligned, phase aligned, and then digitally superposed. Effectively, a multi-aperture digital coherent combining receiver combines multiple inputs to produce a single output signal. This is a practical implementation of multi-aperture coherent combining that uses mature integrated photonics to implement sensitive coherent receivers, narrow linewidth lasers to minimize the effects of laser phase noise, and integrated electronics for implementing the required DSP in real-time. Fortunately, recent advances in the field have enabled the maturation of practical building blocks for optical multi-aperture coherent combining to become a reality for FSO communications [26-28].

This paper is organized as follows. Section 2 discusses the benefits of coherent combining and an algorithm for efficient implemention. Section 3 describes the experimental arrangement for a proof-of-principle fiber-based demonstration of combining four apertures and achieving the same performance as presenting all the power to a single aperture of equivalent collection area. This section also describes the hardware for detecting and digitizing the optical signal and the major DSP operations needed to implement combining and demodulation. Section 4 reports the experimental results of achieving four-aperture combining at various received power levels. Section 5 concludes the paper by summarizing the key technical results.

2. Advantages of multi-aperture receivers

The primary function of the optical front-end for a receiving ground terminal is to collect sufficient usable signal light to close the communication link and efficiently deliver that light to the optical demodulator. The former requires a minimum total collection area while the latter may require that light be coupled directly to a detector or to optical fiber that interfaces with a detector. In particular, the architecture in Fig. 1 relies on coupling light from each aperture into single-mode fiber which then propagates to parallel coherent front ends. A common approach for the efficient coupling of light into a single- or multi-mode receiver is to use adaptive optics (AO) to compensate for the temporally varying atmospheric spatial phase variations across the aperture diameter, *D* [29].

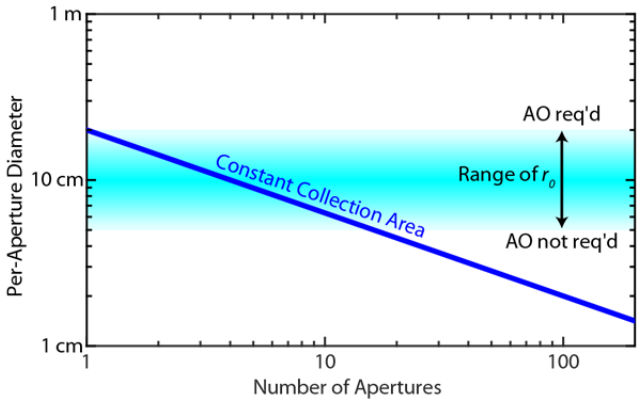

Fig. 2. Constant collection area as a function of the number of apertures. Shaded region is a representative range of the Fried parameter r_0, the $1/e$ correlation length of transverse spatial phase. AO: adaptive optics.

Fig. 2 shows the trades in AO requirements for single-mode coherent receiver coupling for a single aperture system versus a multi-aperture system. The shaded region in Fig. 2 represents a range of realistic Fried parameters, r_0, which measure the phase correlation length of the atmosphere [29]. The larger the ratio of D/r_0, the greater the number of AO elements required to compensate for the spatial phase variations across the aperture. A small Fried parameter corresponds to a turbulent atmosphere and a large Fried parameter to a calm one. For aperture diameters greater than about 20 cm, AO is usually required, and below a diameter of about 5-cm AO is rarely needed for a diffraction-limited single-mode receiver. Increasing the aperture diameter addresses the requirement to collect signal light by increasing the total collection area; however, the collected light will be increasingly difficult to efficiently deliver to a small area detector or single-mode mode fiber [30] and will require the addition of an AO system. Alternatively, the aperture diameter can be fixed at a few centimeters, such that AO is not required, then the number of apertures can be increased until the desired total collection area is achieved. In Fig. 2, the heavy blue line corresponds to aperture geometries with the same total collection area. It then becomes possible to replace a single 20-cm diameter aperture with AO by 16 × 5-cm diameter apertures without AO. It has been argued that the cost for a single aperture as a function of diameter obeys a power law with an exponent of 2.7 (not including the cost of AO or optical signal detection hardware) [12] while increasing the number of apertures is a simple linear relationship.

An array approach also benefits in terms of resilience to atmospheric fading if spatial diversity combining is employed [1, 31, 32]. Atmospheric turbulence can lead to intensity fading on spatial scales similar to r_0. If the array elements are spaced apart by at least a distance of r_0, then the corresponding received signals experience statistically independent and identically distributed fading processes. Consequently, the variance of the fading process after summing the signals is reduced, relative to an individual signal, by a factor equal to the number of apertures in the array. In other words, spatial diversity combining mitigates the deep fades that individual apertures might experience.

Large arrays also have the added benefit of robustness to single element failures and ease of scalability. Any failure of the control of an AO system for a single monolithic telescope would lead to a total loss of communication. Alternatively, an N-element array only loses one Nth of its collection area if one element fails.

There are also several fundamental advantages intrinsic to a multi-aperture ground terminal over a monolithic ground terminal. For example, a ground terminal architecture that supports multiple apertures can be built out over time. An initial deployment may consist of only a few apertures. At a later time the system can be upgraded to add additional apertures and increase the total collection area. It is possible to replace a broken or malfunctioning aperture with minimal cost compared to replacing a single large aperture. A multi-aperture ground terminal also has the potential to support a single user or to support multiple users simultaneously by federating the aperture array. In contrast, single large apertures typically only support a single user at any given time.

3. Coherent combining algorithm

Multi-aperture coherent combining enables using many discrete apertures together to create a large effective aperture. A critical step in the combining process is phase alignment of the different received signals. There are several different techniques for coherently combining signals from different apertures. For example, optical phase-locked loops can be used to coherently combine signals in fiber before detection [10]. However, these techniques have difficulty scaling to a large number of signals due to the amount of analog hardware required. Our technique involves coherently combining signals *after* down-conversion to a near baseband frequency in the RF domain and subsequent digitization (*i.e.*, intradyne detection). In this case, the relative phases of the communication signals can be determined in the RF domain using digital signal processing techniques, thereby avoiding the need to stabilize weak

optical signals to a fraction of a wavelength before combining. Our approach to estimating the relative phases of the different signals relies on computing dot products between pairs of signals, as described below.

The ability to coherently combine signals ($S_1, S_2, \ldots S_N$), where S_i is the complex phasor from the ith aperture, requires being able to accurately determine the relative phase between the N different signals. Suppose that S_1 is used as a reference signal (in practice, the reference signal should be the one with the greatest signal-to-noise ratio). If θ_i is the absolute phase of the ith signal, then the relative phases to be estimated are $\varphi_2, \varphi_3, \ldots, \varphi_N$, where $\varphi_i = \theta_i - \theta_1$. Fig. 3 shows a block diagram of our coherent combining algorithm that uses the calculated φ_i values to determine coherent sum of all the signals.

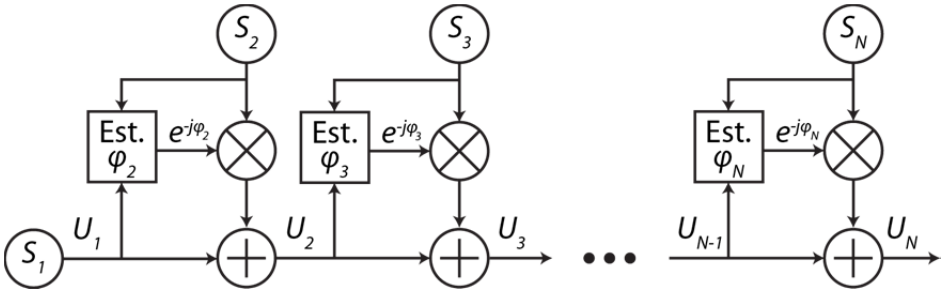

Fig. 3. Coherent combining algorithm block diagram. The φ_i values can be estimated according to Eqns. 1 and 2.

Our estimation technique computes complex dot products between pairs of signals. The complex dot product between two complex signals x and y, each composed of M in-phase and quadrature-phase samples, is defined as

$$\langle x, y \rangle = \sum_{m=1}^{M} x[m] \cdot \overline{y[m]}, \tag{1}$$

where the overbar indicates a complex conjugate. Using M samples from each of the N signals, the relative phases are estimated recursively according to

$$\varphi_i = \arg\left(\langle S_i, U_{i-1} \rangle \right), \tag{2}$$

where $U_1 = S_1$ and

$$U_i = U_{i-1} + e^{-j\varphi_i} S_i, \quad i = 2, \ldots, N. \tag{3}$$

Each U_i has a larger SNR than U_{i-1}, which helps to minimize error in the determination of subsequent values of φ. The coherent combination of all N signals is given by U_N.

The method presented in Fig. 3 and Eqns. 1-3 operates by starting with one signal and coherently combining each subsequent signal with a running coherent sum of all previous signals. This ensures that each subsequent signal is being coherently combined with a signal with a potentially much larger SNR to minimize the phase error of the signal used as the reference in each recurrance. Note that our architecture is distinctly different from either estimating the phase offsets for all the channels in parallel, or a binary tree architecture in which each pair of signals is coherently combined and each pair of coherent sums is then combined and so forth.

4. Experimental arrangement

For the purposes of demonstrating the proposed coherent combining technique, an all fiber experiment was performed in which a multiple aperture array was emulated by a cascade of fiber beam splitters. Fig. 4(a) depicts the transmitter, which consisted of two cascaded Mach-Zehnder modulators (MZMs) that provided data modulation and pulse carving, respectively, for the 11.52-Gb/s single-polarization BPSK waveform. Specifically, biasing the pulse carver modulator at quadrature produced a 50 % return-to-zero pulse shape that helped to reduce inter-symbol interference (ISI) and enabled digital matched filtering in the receiver DSP.

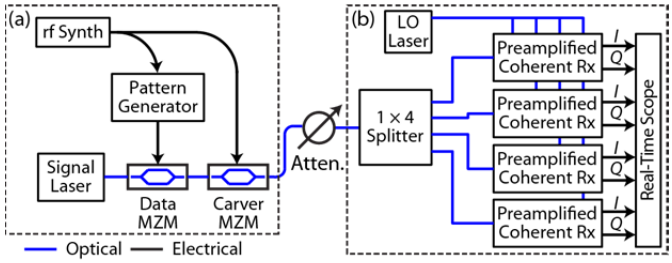

Fig. 4. Experimental arrangement. MZM: Mach-Zehnder modulator.

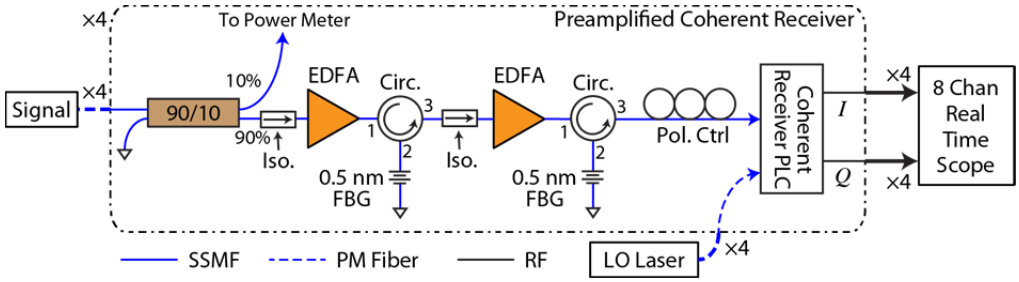

Fig. 5. Detailed schematic of preamplified coherent receiver. Iso: isolator, EDFA: erbium-doped fiber amplifier, Circ: circulator, FBG: fiber Bragg grating, LO: local oscillator, PLC: photonic lightwave circuit.

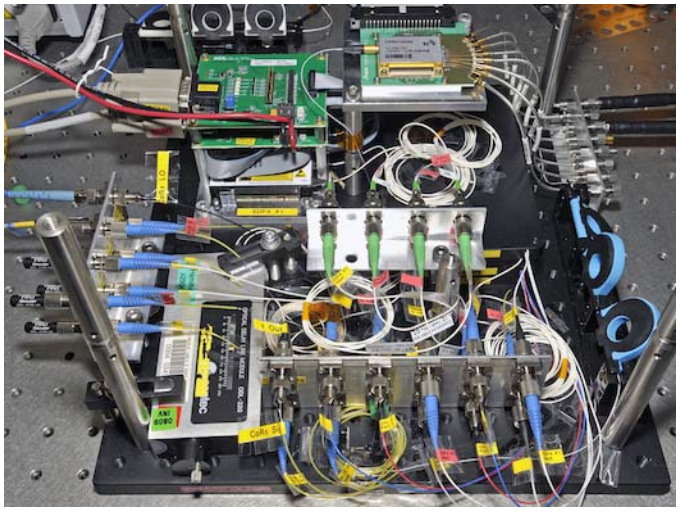

Fig. 6. Photo of a single preamplified coherent receiver mounted on a 12" × 12" optical breadboard.

Fig. 4(b) shows the parallel preamplified coherent receiver architecture. Here, a 1×4 splitter provided input signals to each of the four receivers, and a single local oscillator (LO)

laser provided an LO signal to each receiver. In a real system, separate receiver apertures would feed input signals into each of the coherent receivers. Both the signal and LO laser used were less than 10-kHz linewidth fiber lasers. Fig. 5 shows a detailed schematic of the preamplified coherent receivers used. Every pre-amplified coherent receiver consisted of two stages of erbium-doped fiber amplifiers (EDFAs) and 0.5-nm fiber Bragg gratings (FBGs) for coarse filtering of out-of-band amplified spontaneous emission (ASE) noise from the EDFAs and prevented the second stage EDFA from saturating due to ASE noise from the first stage noise. Here, the 90/10 optical splitter enabled calibrated power measurements into each of the pre-amplified integrated coherent receiver photonic lightwave circuits. An 8-channel 20-GHz real-time oscilloscope acquired samples of the *I* and *Q* components for a single-polarization from each of the receivers. Fig. 6 shows a photo of one of the assembled preamplified coherent receivers mounted on a 12" × 12" optical breadboard that includes additional components used for ease of calibration and testing.

After acquisition of the *I* and *Q* components, several DSP operations needed to be performed to coherently combine the received signals and evaluate BER performance. Fig. 7 shows the major DSP steps used. In particular, coherently combining the signals as early as possible in the DSP chain ensured that a higher SNR is available for the critical steps of frequency estimation and carrier-phase estimation (CPE). Here, we used a data-aided frequency estimator [33] and a feed-forward CPE [34].

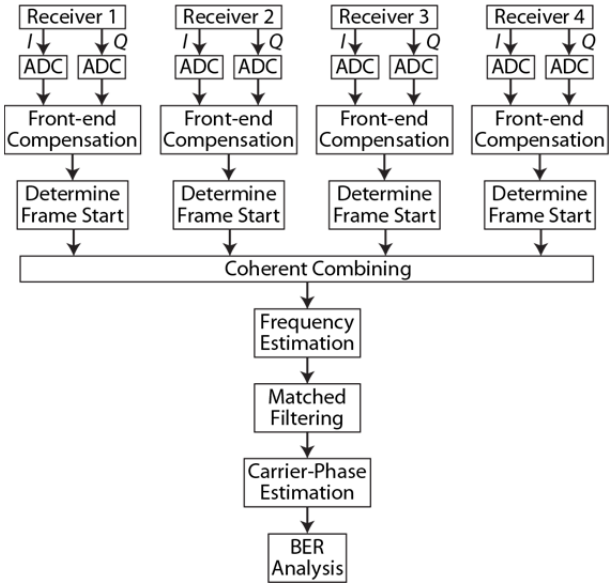

Fig. 7. Digital signal processing steps

The signals were processed in blocks of 64,800 bits, which corresponds to a single DVB-S2 forward-error correction (FEC) codeword [35]. First, each set of digitized *I* and *Q* signals underwent front-end compensation to equalize the *I* and *Q* signal levels and remove *I* and *Q* signal timing skew. Next, a clock recovery algorithm ensured that each signal was aligned modulo a symbol period so that the center location of each symbol was known. Any remaining delay between the received signals is an integer number of symbol periods. The start time of data frames from each of the four receivers was determined by extracting the first 64,800 symbols of each signal, performing carrier-phase estimation, implementing a matched filter, and comparing against a known truth sequence. The relative timing between received signals could also be determined using a pilot sequence or by correlating the signals against each other.

Following Fig. 7, the DSP algorithm coherently combined all of the received signals using the dot product method introduced in Section 3. The relative phases between the signals were assumed to be constant over a duration of 64,800 bits (5.625 μs). In a real system, 5.625 μs would significantly less than a typical atmospheric phase coherence time of approximately 1-10 ms [36]. Next, a frequency estimation algorithm removed the residual beat frequency between the signal and LO [33]. The resulting signal underwent matched filtering using a 50 % return-to-zero (RZ-50) filter to maximize SNR. Next, a CPE algorithm removed the residual relative phase between the signal and LO lasers [34]. The sensitivity performance was then assessed through BER analysis. Individual aperture performance was investigated by omitting the coherent combining step and processing each received signal individually.

5. Multi-aperture coherent combining experimental results

This section summarizes the measured experimental results of four-aperture coherent combining as the input power into the apertures varies. Data acquisitions at each power level consisted of saving 40 MSamples at 40 GSamples/s for the *I* and *Q* components of all four receivers. This resulted in 160 frames of 64,800 bits for a total of 10,368,000 bits for 11.52 GBd BPSK. The relative delays (path length) between the signals seen by each receiver relative to the first receiver were found in DSP to be -24.6 ns (-4.9 m), 7.7 ns (1.5 m), and 1.9 ns (0.4 m), which were due to differences in fiber pigtail length. The advantages of operating in the digitized RF domain are clearly manifested in this case. To perform such combining with an analog optical approach would require less than 150 nm precision length control with more than 5 meters of dynamic range.

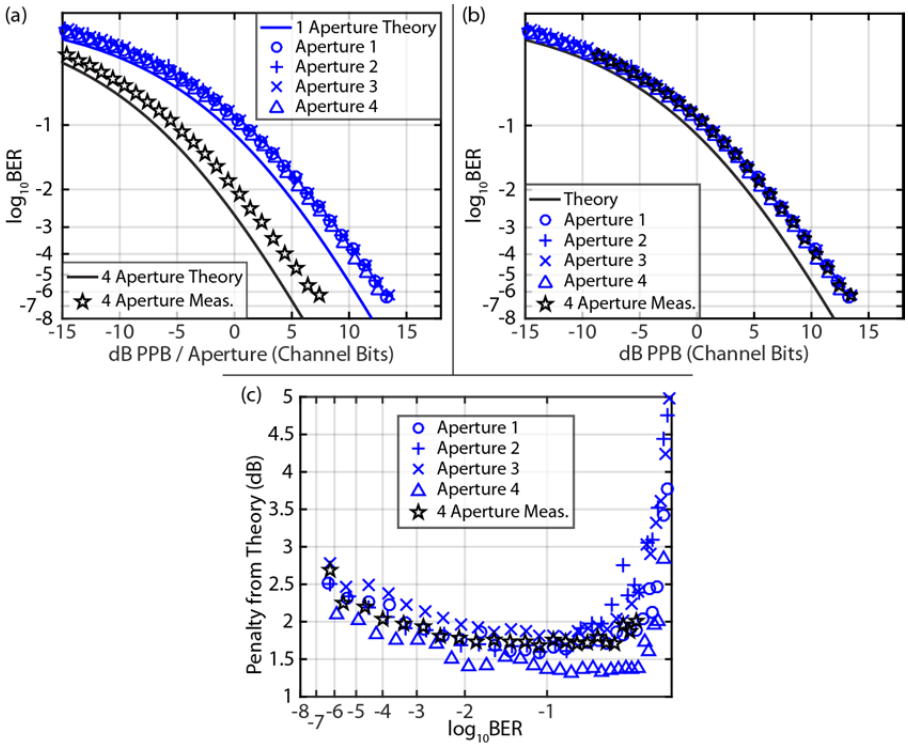

Fig. 8. Log BER vs. (a) dB PPB per aperture and (b) dB PPB for each aperture signal and the coherent combination of all four signals. (c) Penalty from theory vs. log BER.

Fig. 8(a) shows that all four receivers (blue symbols) had almost identical sensitivity performance. Note that the performance starts to degrade significantly from theory

around -6 dB photon-per-bit (PPB), which is attributable to the CPE algorithm implementation being unable to efficiently determine the residual frequency offset between the signal and LO at such low power levels.

Coherent combining using DSP yielded an improved sensitivity of 6-dB in terms of dB PPB per aperture. The improvement in the low power regime is a result of implementing the coherent combining as soon as possible in the DSP processing chain, which provides a higher SNR signal to the CPE algorithm than could be provided by any of the signals individually. Fig. 8(b) shows the data from Fig. 8(a) with the *x*-axis normalized to total combined dB PPB instead of dB PPB per aperture. Note that the DSP-based coherent combining result is nearly identical in performance to each single receiver with the same received power. Received power levels that result in BERs between 0.05 and 0.20 are of interest for power starved FSO communications since strong FEC enables error free results after decoding [1, 10, 11].

Fig. 8(c) shows the penalty from theory vs. BER for the individual receivers and for DSP-based coherent combining. The penalties from theory of the individual receivers are within approximately 0.5 dB of each other. The slight difference in performance of the four receivers can likely be attributed to slight differences in connector losses leading into their respective preamplifiers. Receivers with fully spliced components instead of FC/PC connectors should result in improved performance consistency between the receivers. Individual receiver penalty from theory ranged from approximately 2.5 dB to approximately 1.5 dB across the range of BER evaluated. The penalty for coherent combining is approximately the average penalty of the individual receivers. Note that the DSP-based coherent combining result tracks closely with the performance of the individual receivers in terms of dB PPB per receiver. This indicates that there is a negligible penalty as a result of the coherent combining.

Fig. 9 shows the achieved performance gain in dB as a function of dB PPB per aperture for the DSP-based coherent combining result. There is a 6-dB performance gain through received power levels as low as -15 dB PPB per aperture. Any deviation of the measured data above the theoretical 6-dB performance improvement is due to the offline processing of a finite number of bits at each power level.

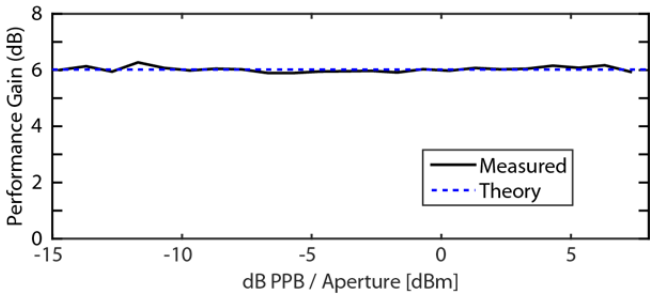

Fig. 9. Performance gain vs. received power after coherently combining signals from 4 apertures.

6. Conclusion

Reducing the space-side SWaP of optical communication links to Earth is a major goal for the free-space optical community. An efficient means of accomplishing this goal is to increase ground station collection area. The conventional approach is to increase the diameter of a single-aperture ground station. In contrast, our approach is to coherently combine signals from many smaller apertures to create a single large effective aperture.

In this work, we presented a ground terminal receiver architecture that relies on the coherent combining of signals detected from different apertures. A DSP-based coherent combining algorithm has been presented wherein we show that coherently combining signals as soon as possible in the DSP processing chain is advantageous due to the higher SNR

available to the CPE algorithm. Our experiment successfully demonstrated lossless coherent combining of four digital coherent receivers with performance within 2 dB of theory.

The ability to coherently combine signals from multiple apertures opens up a new tradespace for ground station design. In particular, it may be more cost effective to use multiple apertures instead of a single large aperture due to the difference in cost scaling. Furthermore, the use of multiple apertures adds additional benefits such as the ability to mitigate atmospheric fading with spatial diversity, to use small aperture size to reduce or eliminate AO complexity, to increment ground station collection area over time, to reduce cost, to remove a single point of failure, and to enable support for simultaneous communications links by federating the array to multiple targets. These benefits, combined with the experimental results presented in this paper, strongly suggest that a multi-aperture coherent receiver approach should be considered for future ground stations.

This work was sponsored by the Assistant Secretary of Defense for Research and Engineering under Air Force Contract #FA8721-05-C-0002. Opinions, interpretations, conclusions, and recommendations are those of the authors and are not necessarily endorsed by the United States Government.